

Modeling Colored Impulsive Noise by Markov Chains and Alpha-Stable Processes

Ahmed Mahmood and Mandar Chitre

Acoustic Research Laboratory, Tropical Marine Science Institute,

National University of Singapore, Singapore 119222

e-mail: {tmsahme, mandar}@nus.edu.sg

Abstract—We present a novel method of modeling ambient noise in warm shallow underwater channels. Due to large snapping shrimp populaces inhabiting these regions, the noise process is known to be impulsive and bursty (colored). Conventionally, researchers have used white noise models to simulate snapping shrimp noise. Though efficient in portraying the amplitude statistics, these models fail to represent the burstiness encountered in practical observations. We offer insights into the dependence between recorded noise samples. Scatter plots of closely spaced observations are shown to have near-elliptical geometries. Using this observation and the fact that stable distributions model outliers very well, we propose a memory model based on stable α -sub-Gaussian distributions. The new model offers a better match to empirical data in comparison to white and colored noise models currently employed in the literature.

I. INTRODUCTION

Noise encountered in warm shallow underwater channels is typically impulsive in nature [1]. This phenomenon is primarily attributed to the snapping shrimp. These underwater dwellers inhabit warm coastal regions around the world and are generally found in large droves [2]. The snapping shrimp has a remarkably distinctive large front pincer which has the potential of generating large surges of pressure (or snaps) by cavitating bubbles. Divers and acoustic systems operating in the vicinity of a snapping shrimp populace will hear crackling in the background. Peak-to-peak levels of a single snap have been recorded to be as high as 190 dB re 1 μ Pa at 1 m from the position of the shrimp [2].

In the literature, various noise models have been introduced to model impulsive noise [1], [3]–[5]. These are based on heavy-tailed distributions due to the latter’s tendency of generating outliers (impulses) with non-negligible probability. In [1], [6], the amplitude distribution of snapping shrimp noise has been shown to be tracked closely by symmetric α -stable ($S\alpha S$) distributions. From a theoretical perspective, $S\alpha S$ random variables and vectors offer attractive limiting and stability properties [7], [8]. This in turn allows mathematical tractability for a plenitude of processing schemes [3]. We therefore restrict our work to $S\alpha S$ distributions.

We can divide impulsive noise models in to two broad categories: *white* and *colored* noise models. If a noise process is white, its time samples are independent and identically distributed (IID) random variables, each of which has a *symmetric* distribution [9]. Examples of commonly employed white impulsive noise models are the Gaussian-Bernoulli-

Gaussian (GBG) model [4], the Middleton class models [10] and the white symmetric α -stable ($WS\alpha SN$) model [3], [6]. Though ‘whiteness’ typically refers to a flat power spectral density (PSD), it does not extend to the $WS\alpha SN$ case as second order moments of $S\alpha S$ distributions are infinite [8]. On the other hand, a colored noise process does not have a flat PSD [9]. This implies that its samples are correlated in time and therefore the process depicts memory. This impacts the transience of an impulse, which tends to linger on for a number of adjacent samples.

Markov chains are abundantly used to model various real world scenarios [11]. For example, amongst many possible configurations, a channel with white noise may be represented by a single state with its self-transition probability equal to one. The state signifies that the noise samples are chosen from a certain probability density function (PDF). If the noise process has memory, one can add more states and transition paths to model this adequately. Following this line of reasoning, various colored impulsive noise models have been introduced in the literature [12], [13]. In [12], building on the white GBG model, the authors propose a two-state Markov chain to introduce dependency between the occurrence of good (white Gaussian noise) and bad (bursty) channels and term this as the Markov-Gaussian (MG) model. In [13], the authors take advantage of the weighted-sum structure of the Middleton class-A PDF [10] to construct a multi-state Markov model. A single parameter is introduced that controls the transitional probability between the states. The model is justly termed as the Markov-Middleton (MM) model.

In this paper, we highlight the pros and cons of $WS\alpha SN$, the MG and the MM models when employed for snapping shrimp noise. We show how these models fail to address the dependence between empirical noise samples and propose a novel memory model based on the stable α -sub-Gaussian distribution to address this problem.

As highlighted previously, a noise process is termed ‘impulsive’ if one observes a significant number of outliers in its realizations. If the noise process is colored, then due to the implicit memory of the channel, any impulse would affect subsequent time samples. One would therefore see clustering of many outliers which in turn are called bursts. In [12], [13], the authors justly state their works to model ‘bursty impulsive noise’. We adhere to these definitions in our work.

This paper is organized as follows: In Section II, we

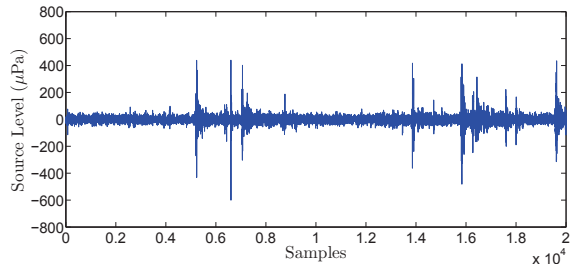


Fig. 1. A realization of snapping shrimp noise.

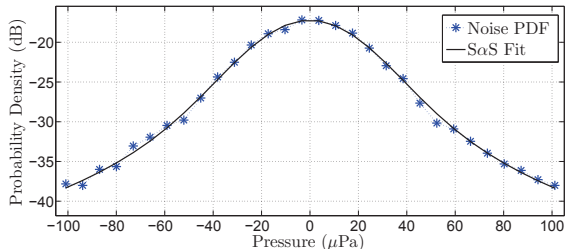


Fig. 2. Amplitude distribution of snapping shrimp noise and an ML fitted SαS PDF.

present the motivation for our work and offer insights into the dependence between adjacent samples in a snapping shrimp noise process. In Section III, we briefly summarize properties of multivariate α -sub-Gaussian distributions. The noise model is proposed in Section IV and is compared with the MG and MM models. In Section V, we show how the parameters of the noise model can be tuned to empirical data. We analyze the proposed model in Section VI and wrap up by presenting the conclusions in Section VII.

II. MOTIVATION & PROBLEM STATEMENT

One issue with practical noise is that it is seldom white. To highlight this, we plot a realization of snapping shrimp noise in Fig. 1. This data set was recorded in the coastal regions of Singapore. One can clearly see that the realization is impulsive as it has a significant number of outliers. It is also colored, as seen by the clustering of impulses. In Fig. 2 we plot the empirical PDF of the noise realization in Fig. 1. We also plot the corresponding maximum-likelihood (ML) SαS PDF fit for comparison. Clearly, the empirical amplitude distribution is tracked well by the SαS PDF. In Fig. 3, we plot a WSαSN realization corresponding to the evaluated SαS PDF in Fig. 2. Despite the similarity of their amplitude distributions, the bursty nature of the observations in Fig. 1 is not reflected in Fig. 3. Therefore, the WSαSN process models the impulsiveness of the noise data but *does not* reflect the burstiness within it.

Denoting the i^{th} received observation in Figs. 1 & 3 by x_i , we present the corresponding scatter plots between x_{i+1} and x_i in Fig. 4. This offers a powerful visual of the dependence structure between immediately adjacent samples of the WSαSN and snapping shrimp noise processes, respectively.

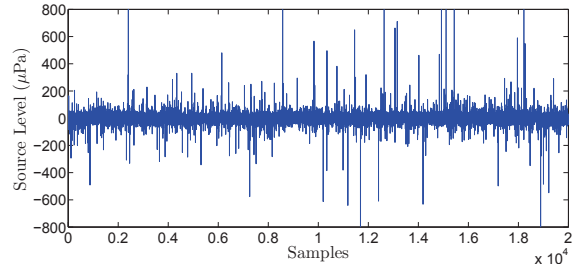


Fig. 3. A realization of WSαSN.

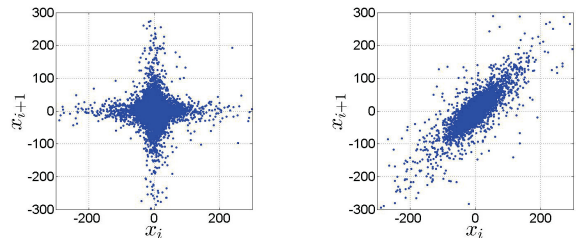


Fig. 4. Unit delay scatter plots of WSαSN (left) and of snapping shrimp noise data (right).

One cannot help notice a near-elliptical geometry in the latter case. Clearly, WSαSN fails to model this characteristic by offering us a four-tailed geometry instead. As shown in Fig. 5, higher-order delay scatter plots for snapping shrimp data also offer us near-elliptic geometries.

It is already known that the empirical amplitude distribution of snapping shrimp noise is followed well by SαS distributions [1]. Now we also know that the dependence between delayed samples follows near-elliptic geometries. A good model should depict both these traits. We introduce concepts that help us understand how to do this next.

III. α -SUB-GAUSSIAN RANDOM VECTORS

A random vector \vec{X} is *symmetric* if its PDF $f_{\vec{X}}(\mathbf{x})$ satisfies the expression

$$f_{\vec{X}}(\mathbf{x}) = f_{\vec{X}}(-\mathbf{x}). \quad (1)$$

If \vec{X} also satisfies

$$c\vec{X} \stackrel{d}{=} \sum_i a_i \vec{X}^{(k)}, \quad (2)$$

it is called SαS. Here $a_i, c \in \mathbb{R}$ and $\vec{X}^{(k)} \forall k \in \mathbb{Z}^+$ are independent and identically distributed (IID) copies of \vec{X} [7], [8]. The symbol $\stackrel{d}{=}$ implies *equality in distribution* [8]. The expression in (2) highlights the fact that any *linear* combination of $\vec{X}^{(i)}$ will have a similar (albeit scaled) distribution as the individual copies. This, in essence, is the *stability property* for SαS random vectors [8]. It should be noted that if \vec{X} is a symmetric (zero-mean) Gaussian random vector, then it also satisfies (2). Therefore, a symmetric Gaussian random vector is SαS as well. Another well-known member of the SαS family is the zero-median Cauchy distribution.

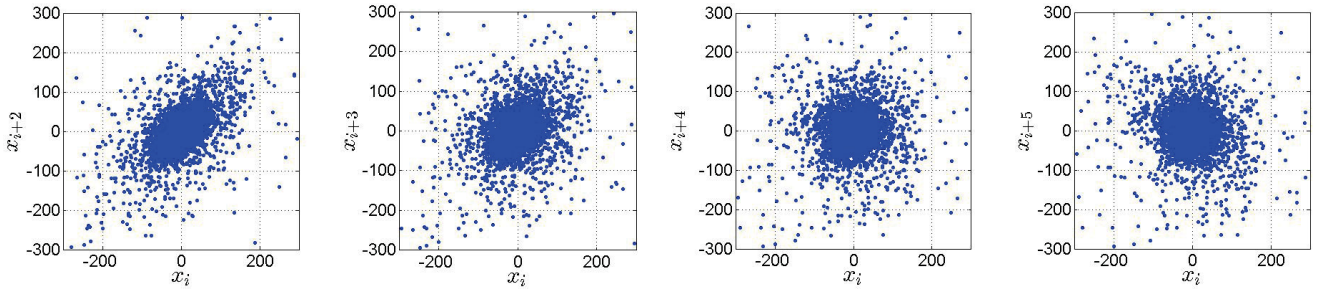


Fig. 5. Scatter plots between noise observations with varying delay.

We are interested in a certain subclass of the S α S family: the α -sub-Gaussian distribution. As highlighted by their name, these distributions share additional properties with their Gaussian counterparts [7], [8]. In fact, any α -sub-Gaussian random vector $\vec{X} = [X_1, X_2, \dots, X_n]^T$ can be expressed in terms of a Gaussian vector $\vec{G} = [G_1, G_2, \dots, G_n]^T$ by

$$\vec{X} = A^{1/2} \vec{G}, \quad (3)$$

where $n \in \mathbb{Z}^+$, A is a totally right-skewed *stable random variable* and $\vec{G} \sim \mathcal{N}(\mathbf{0}, \mathbf{R})$ [7], [8]. Here, $\mathbf{0}$ is the $n \times 1$ all-zero vector and $\mathbf{R} = [r_{ij}]$ is the $n \times n$ covariance matrix of \vec{G} . A consequence of the relationship in (3) is that \vec{X} has an elliptical distribution due to the underlying \vec{G} , but it is heavy-tailed as well [8].

With the exception of the Gaussian case, all S α S distributions are heavy-tailed (algebraic tails) [7], [8]. This allows them to model impulsive data very well. A downside is that with the exception of the Gaussian and Cauchy cases, the PDF of an S α S random vector does not exist in closed-form. One therefore needs to revert to other equivalent representations for mathematical tractability.

For the α -sub-Gaussian family, the characteristic function (CF) fortunately offers us a nice closed-form. If \vec{X} is α -sub-Gaussian, its CF is given by

$$\Phi_{\vec{X}}(\boldsymbol{\theta}) = E[\exp(j\boldsymbol{\theta}^T \mathbf{x})] = \exp\left(-\left(\frac{1}{2}\boldsymbol{\theta}^T \mathbf{R} \boldsymbol{\theta}\right)^{\frac{\alpha}{2}}\right), \quad (4)$$

where $\boldsymbol{\theta} = [\theta_1, \theta_2, \dots, \theta_n]^T$ and the *characteristic exponent* $\alpha \in (0, 2]$ controls the heaviness of the tails of the distribution [7], [8]. The lower the value of α , the heavier the tails. For $\alpha = 1$ and $\alpha = 2$, (4) corresponds to the CF of an elliptic Cauchy and a Gaussian distribution, respectively. As the CF is the Fourier transform of $f_{\vec{X}}(\mathbf{x})$, there is a one-to-one relationship between the both of them. Therefore, (4) completely represents the statistics of \vec{X} . One notes that the CF of \vec{X} is parameterized by α and \mathbf{R} . Moreover, (3) holds for all $\alpha < 2$.

The marginal CF of X_i may be evaluated from (4) by merely substituting $\theta_k = 0 \forall k \neq i$. This results in

$$\Phi_{X_i}(\theta) = \exp\left(-|\sqrt{r_{ii}/2}|^\alpha |\theta|^\alpha\right). \quad (5)$$

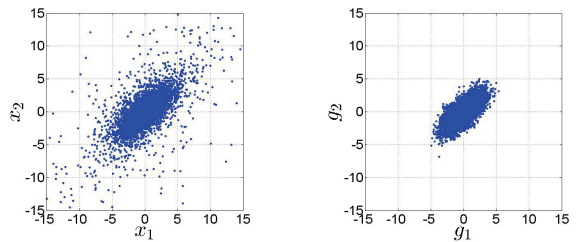


Fig. 6. Dependence structures: a bivariate α -sub-Gaussian random vector with $\alpha = 1.5$ (left) and the underlying symmetric Gaussian random vector (right).

The CF in (5) is that of a S α S *random variable* where $\delta_i = |\sqrt{r_{ii}/2}|$ is the *scale* of the corresponding PDF [8]. Expanding this result, if \vec{X} is α -sub-Gaussian, then we note that any pair of $k < n$ distinct random variables in the set $\{X_1, X_2, \dots, X_n\}$ also results in a α -sub-Gaussian random vector. The corresponding CF may be acquired from (4) by equating the irrelevant elements of $\boldsymbol{\theta}$ to zero.

As an example, in Fig. 6, we highlight the dependence between the components of $\vec{X} = [x_1, x_2]^T$ for the bivariate case by generating multiple independent outcomes and presenting the scatter plot between the components. We do the same for the underlying \vec{G} . The plots are constructed for $\alpha = 1.5$ and

$$\mathbf{R} = \begin{bmatrix} 1 & 0.7 \\ 0.7 & 1 \end{bmatrix}. \quad (6)$$

Clearly, the scatter plot of \vec{X} follows the elliptic geometry of \vec{G} . However, as expected, it offers more outliers. By varying α one can control the probability of observing outliers in \vec{X} .

Now that we know how one can construct elliptical distributions while still being heavy-tailed S α S, we discuss the noise model next.

IV. THE NOISE MODEL

A. Stationary α -Sub-Gaussian Noise with Memory

Let us define m as the *memory order* of the noise process and the $(m + 1)$ -dimensional random vector $\vec{X}_{t,m} = [X_{t-m}, X_{t-m+1}, \dots, X_t]^T$ as a window of the current and m immediate observations at sampling index $t \in \mathbb{Z}$. As established previously in the text, we want $\vec{X}_{t,m}$ to have

an elliptical distribution. Additionally, it should also be S α S so that it may model the empirical amplitude distribution of snapping shrimp noise. It should therefore be an α -sub-Gaussian random vector.

From (3), the relationship between $\vec{X}_{t,m}$ and its underlying Gaussian vector $\vec{G}_{t,m}$ is given by

$$\vec{X}_{t,m} = A_t^{1/2} \vec{G}_{t,m}. \quad (7)$$

From (4), the joint-CF of $\vec{X}_{t,m}$ is

$$\Phi_{\vec{X}_{t,m}}(\boldsymbol{\theta}) = \exp\left(-\left(\frac{1}{2}\boldsymbol{\theta}^T \mathbf{R}_{t,m} \boldsymbol{\theta}\right)^{\frac{\alpha}{2}}\right), \quad (8)$$

where $\mathbf{R}_{t,m}$ is the $(m+1) \times (m+1)$ covariance matrix of $\vec{G}_{t,m}$. One does note that if $\mathbf{R}_{t,m}$ is independent of t , then the CF in (9) (and therefore the corresponding PDF) does not vary with t . Consequently, the noise process $X_t \forall t \in \mathbb{Z}$ will be *stationary*. By restricting the model to this category, (8) reduces to

$$\Phi_{\vec{X}_{t,m}}(\boldsymbol{\theta}) = \Phi_{\vec{X}_m}(\boldsymbol{\theta}) = \exp\left(-\left(\frac{1}{2}\boldsymbol{\theta}^T \mathbf{R}_m \boldsymbol{\theta}\right)^{\frac{\alpha}{2}}\right), \quad (9)$$

where $\mathbf{R}_m = [r_{ij}]$. The CF in (9) then corresponds to any *ordered* $m+1$ *immediately adjacent* samples in the noise process $X_t \forall t \in \mathbb{Z}$.

To maintain consistency in (9), \mathbf{R}_m has the following properties:

- 1) The diagonal elements of \mathbf{R}_m are equal, i.e., $r_{ii} = 2\delta^2 \forall i \in \{1, 2, \dots, m+1\}$. This implies that $X_t \forall t \in \mathbb{Z}$ are *identical* random variables with scale parameter δ . Therefore, from (5) and (9), the CF of X_t is given by

$$\Phi_X(\theta) = \exp(-\delta^\alpha |\theta|^\alpha). \quad (10)$$

- 2) The k^{th} off-diagonal elements are equal as well. Mathematically, $r_{i,i+k} = r_{j,j+k} \forall k \in \{1, 2, \dots, m\}$ and $i, j \in \{1, 2, \dots, m-k+1\}$.
- 3) As \mathbf{R}_m is a *real* covariance matrix, it is positive semi-definite and thus symmetric, i.e., $\mathbf{R}_m = \mathbf{R}_m^T$ [11]. We note that only r_{ij} for $j \geq i$ are sufficient to construct \mathbf{R}_m as $r_{ij} = r_{ji} \forall i, j \in \{1, 2, \dots, m\}$.

To deem the model effective, the parameters α and \mathbf{R}_m need to be evaluated. Due to the constraints of \mathbf{R}_m , it is not hard to see that \mathbf{R}_m is a *symmetric Toeplitz matrix* and can be constructed by knowing just one of its rows or columns, i.e., $m+1$ elements. Therefore, inclusive of m and α , the model is defined by $m+3$ parameters.

For brevity, we term the above model as the α SGN(m) model, which spells out to be *stationary α -sub-Gaussian noise with memory order m* .

B. Markov Chain Representation

Before we show how the α SGN(m) model can be represented by a Markov chain, it is pertinent to summarize characteristics of colored impulsive noise models in the literature and see how they differ from the proposed model.

In [12] and [13], the authors introduce the MG and the MM models, respectively, to model bursty impulsive noise.

With a few exceptions, these models are similar and share the following characteristics:

- 1) The MG and MM models are derived from the GBG and the Markov Class-A PDF, respectively. Each of these PDFs can be expressed as a weighted sum of zero-mean Gaussian PDFs with different variances. For the GBG distribution, the total number of elements in the sum is two.
- 2) Both models can be represented by a finite-state Markov chain, where each state represents an elemental Gaussian PDF from which random variates are generated.
- 3) The number of states for the MG model is two, while that for the MM model depends on the number of terms considered in the underlying Middleton Class A PDF.
- 4) There is a direct path from any one state to any other state.
- 5) Within one state, the random variates generated are IID Gaussian.
- 6) Transitions between different states occur *rarely*. If the new state corresponds to a Gaussian PDF with a larger variance, the noise samples that follow appear more impulsive and bursty with respect to those in the previous state.

Due to the definition of their state space, one notes that the samples in a MG and MM noise process will always be *independent* Gaussian random variables. Consequently, they do not depict the elliptical geometries shown in Figs. 4 and 5. This is why we do not consider them for modeling snapping shrimp noise. Also, as an α -sub-Gaussian PDF cannot be expressed as a countable sum of weighted Gaussian PDFs (it can be represented as an integral though), the Markov chain representation of the α SGN(m) process is very much different.

We now discuss how an α SGN(m) process can be represented by a Markov chain. We denote the PDF corresponding to the CF in (9) as $f_{\vec{X}_m}(\cdot)$, where $\vec{X}_m = [X_1, X_2, \dots, X_{m+1}]^T$. To generate a realization of α SGN(m), one has to output the t^{th} sample x_t from the conditional PDF

$$f_{X_{m+1}|\vec{X}_{m-1}}(x_t) = \frac{f_{\vec{X}_m}(\mathbf{x}_{t,m})}{f_{\vec{X}_{m-1}}(\mathbf{x}_{t-1,m-1})}, \quad (11)$$

where $\mathbf{x}_{t,m} \in \mathbb{R}^{m+1}$ is a sample outcome of $\vec{X}_{t,m}$. In practical scenarios, x_t and thus $\mathbf{x}_{t,m}$, will take over a finite set of values due to digital sampling. One can then discretize (11) to generate the conditional probability

$$P[X_{m+1} = x_t | \vec{X}_{m-1} = \mathbf{x}_{t-1,m-1}] = \frac{P[\vec{X}_m = \mathbf{x}_{t,m}]}{P[\vec{X}_{m-1} = \mathbf{x}_{t-1,m-1}]}. \quad (12)$$

The process in (12) is clearly a stationary Markov process with order m . We define the state space of the Markov chain as the set of all possible m -tuples $\mathbf{x}_{t-1,m-1}$ can take after discretization and note it to be finite. The cardinality of the state space depends on the resolution of the discretizing process. Denoting the state at time t as $s_t = \mathbf{x}_{t,m-1}$, the one-step transition from s_{t-1} to s_t is given by (12).

In contrast to the Markov chain representation of the MG and MM processes, a state represents m immediately adjacent samples of the $\alpha\text{SGN}(m)$ noise process. One notes that due to the overlap of elements in $\mathbf{x}_{t-1,m-1}$ and $\mathbf{x}_{t,m-1}$, not all states are connected. Also, the probability for remaining in a certain state is very small, as this implies $\mathbf{x}_{t,m-1}$ does not vary with t .

We have defined and highlighted various properties of the $\alpha\text{SGN}(m)$ model. The next step is to know how to estimate its parameters.

V. ESTIMATION OF PARAMETERS

In the case of $\text{WS}\alpha\text{SN}$, the received observations are IID with CF given by (10). Therefore, α and δ are the only parameters that need to be estimated. In the literature, various robust mechanisms have been introduced to do this. A summary of these mechanisms is presented in [8], [14].

For the $\alpha\text{SGN}(m)$ model, estimation of its parameters can be done in two steps:

- 1) Evaluate α and δ as one would in the case of $\text{WS}\alpha\text{SN}$.
- 2) Using the estimated values $\hat{\alpha}$ and $\hat{\delta}$ (with obvious notation), one may evaluate a row or column of \mathbf{R}_m . Due to the latter's structure, one can then proceed to construct the entire matrix.

The first step is validated by noting that estimators in a white noise process only take sample values under consideration and not the indices. Therefore, such estimates of α and δ are equivalent if one evaluates them from an $\alpha\text{SGN}(m)$ realization or a whitened version of $\alpha\text{SGN}(m)$ achieved by randomly interleaving the samples.

For the second step, given $[X_1, X_2]^T$ is a $\text{S}\alpha\text{S}$ random vector, we have from [7]:

$$\frac{E[X_1 X_2^{(p-1)}]}{E[|X_2|^p]} = \frac{[X_1, X_2]_\alpha}{\delta_2^\alpha} \quad (13)$$

for $\alpha > 1$ and $1 \leq p < \alpha$. The term δ_2 is the scale parameter of X_2 and $[X_1, X_2]_\alpha$ is the *covariation* between X_1 and X_2 [7], [8]. Also, $X_2^{(p-1)} = \text{sign}(X_2)|X_2|^{p-1}$, where $\text{sign}(\cdot)$ is the sign operator. If $[X_1, X_2]^T$ is further constrained to be an α -sub-Gaussian random vector with CF given by (4), we have

$$[X_1, X_2]_\alpha = 2^{-\alpha/2} r_{12} r_{22}^{\alpha/2-1}. \quad (14)$$

We now interpret (13) and (14) in terms of the parameters in the $\alpha\text{SGN}(m)$ model. As discussed previously, due to $\vec{X}_{t,m}$ being an α -sub-Gaussian vector, any pair of two *distinct* elements in $\vec{X}_{t,m}$ is a bivariate α -sub-Gaussian random vector. By taking the constraints on \mathbf{R}_m under consideration, (13) can be written as

$$\frac{E[X_{t-k} X_t^{(p-1)}]}{E[|X_t|^p]} = \frac{[X_{t-k}, X_t]_\alpha}{\delta^\alpha}, \quad (15)$$

where $k \in \{1, 2, \dots, m\}$, $t \in \mathbb{Z}$ and

$$\begin{aligned} [X_{t-k}, X_t]_\alpha &= 2^{-\alpha/2} r_{t-k,t} r_{tt}^{\alpha/2-1} \\ &= \frac{1}{2} r_{t-k,t} \delta^{\alpha-2}. \end{aligned} \quad (16)$$

TABLE I
PARAMETERS OF THE $\alpha\text{SGN}(m)$ MODEL TUNED TO TWO DIFFERENT DATASETS \mathcal{D}_1 AND \mathcal{D}_2 FOR $m \in \{0, 1, 2, 3, 4\}$.

		$\frac{\hat{r}_{1,1+k}}{2\hat{\delta}^2}$	
		\mathcal{D}_1	\mathcal{D}_2
k	$\hat{\alpha}$	1.715	1.623
	$\hat{\delta}$	10.263	11.866
	0	1.000	1.000
	1	0.621	0.644
	2	0.237	0.244
	3	0.161	0.119
	4	-0.054	-0.001

Substituting (16) in (15) and simplifying, we get

$$r_{t-k,t} = \frac{E[X_{t-k} X_t^{(p-1)}]}{E[|X_t|^p]} 2\delta^2. \quad (17)$$

As the $\alpha\text{SGN}(m)$ process is stationary, $r_{t-k,t} = r_{1,1+k}$. Also, as the expectation terms in (17) are finite for $1 \leq p < \alpha$ [7], [8] and the random process X_t is ergodic, we may write the estimate of $r_{1,1+k} \forall k \in \{1, 2, \dots, m\}$ as

$$\hat{r}_{1,1+k} = \frac{\frac{1}{L-k} \sum_{t=k+1}^L x_{t-k} x_t^{(p-1)}}{\frac{1}{L} \sum_{t=1}^L |x_t|^p} 2\hat{\delta}^2, \quad (18)$$

where $x_t \forall t \in \{1, 2, \dots, L\}$ are the observations in a noise realization and $1 \leq p < \alpha$. The estimator in (18) is realistic as $\alpha \geq 1.5$ in practical scenarios [1], [6].

One notes that (18) is a *consistent* estimator of $r_{1,1+k} \forall k \in \{1, 2, \dots, m\}$ if $\hat{\delta}$ is a *consistent* estimate of δ [15]. Initially, one may note that (17) is independent of α . However, it is implicitly accounted for due to the bound $1 \leq p < \alpha$. In [8], the authors suggest using $p = 1$ as (18) simplifies to the computationally desirable form

$$\hat{r}_{1,1+k} = \frac{\frac{1}{L-k+1} \sum_{t=k}^L x_{t-k} \text{sign}(x_t)}{\frac{1}{L} \sum_{t=1}^L |x_t|} 2\hat{\delta}^2. \quad (19)$$

From (19) we can estimate the first row of \mathbf{R}_m , and therefore the entire matrix.

VI. ANALYSIS OF THE $\alpha\text{SGN}(m)$ MODEL

We now demonstrate how the $\alpha\text{SGN}(m)$ process models snapping shrimp data after tuning the corresponding parameters with empirical observations. We present noise realizations and delay scatter plots to achieve this end. We consider two empirical datasets \mathcal{D}_1 and \mathcal{D}_2 , each with 20000 samples, recorded during the ROMANIS 2014 experiments in Singapore. In Table I, we present the values of tuned parameters of the $\alpha\text{SGN}(m)$ model with respect to \mathcal{D}_1 and \mathcal{D}_2 . For $\hat{\alpha}$ and $\hat{\delta}$, we invoke the ML estimator (MLE) which is known to be consistent [14]. The estimate $\frac{\hat{r}_{1,1+k}}{2\hat{\delta}^2}$ is that of the

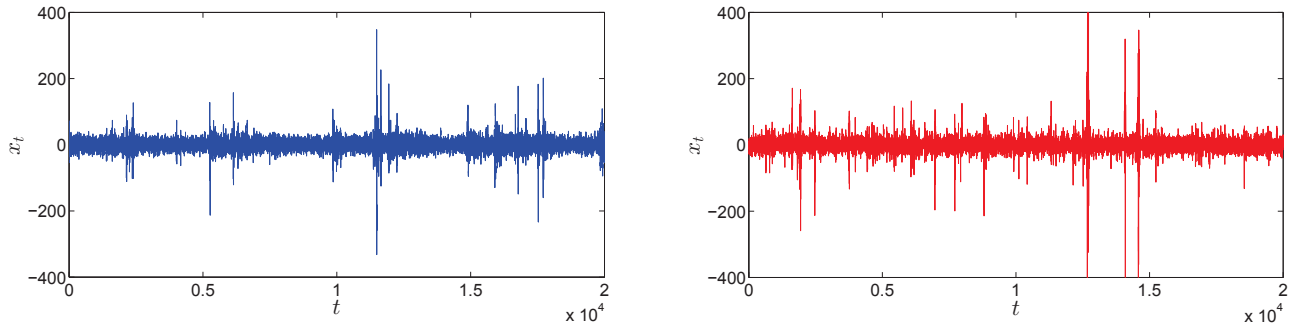


Fig. 7. For \mathcal{D}_1 : Empirical observations (left) and a realization of $\alpha\text{SGN}(4)$ (right) with tuned parameters.

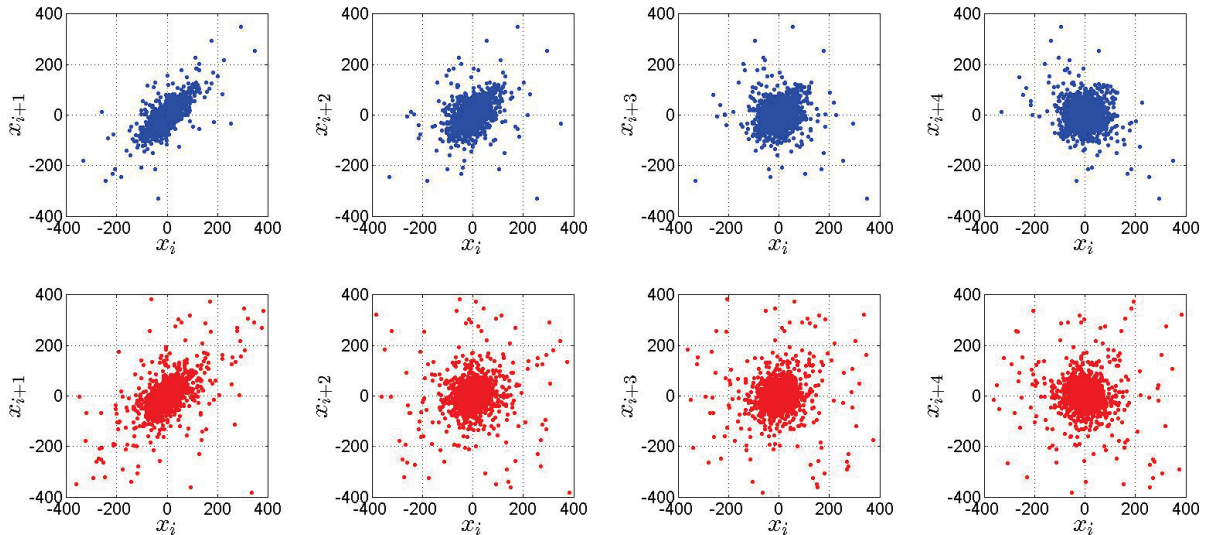


Fig. 8. For \mathcal{D}_1 : Delay scatter plots (top row) and those of the tuned $\alpha\text{SGN}(4)$ realization (bottom row).

correlation coefficient of the underlying Gaussian process. This is evaluated via (19). We note that \mathcal{D}_2 is more impulsive than \mathcal{D}_1 , hence the lower $\hat{\alpha}$. These data sets represent moderate to severe levels of snapping shrimp noise.

In Fig. 7, we present \mathcal{D}_1 and a noise realization from the corresponding tuned $\alpha\text{SGN}(4)$ process. As expected, one can see the impulses cluster together in the latter, unlike the white noise realization in Fig. 3. The same can be observed for \mathcal{D}_2 and its tuned $\alpha\text{SGN}(4)$ realization in Fig. 9. To construct an $\alpha\text{SGN}(m)$ realization, one may generate the *random variate* x_t by numerically evaluating the conditional density in (11) and applying rejection sampling [11].

Delay scatter plots of closely spaced samples offer us a more detailed insight into the burstiness of snapping shrimp data. In Fig. 8, we present them for \mathcal{D}_1 (top row) and the corresponding $\alpha\text{SGN}(4)$ realization (bottom row) up until a delay order of four. One can see how the elliptical geometries of the $\alpha\text{SGN}(4)$ realization track those of \mathcal{D}_1 . Similar observations can be made in Fig. 10 for \mathcal{D}_2 (top row) and its associated $\alpha\text{SGN}(4)$ realization (bottom row). In comparison to the $\text{WS}\alpha\text{SN}$ scatter

plot in Fig. 4, clearly the $\alpha\text{SGN}(4)$ process offers a better fit to the dependence structure observed in empirical data.

VII. CONCLUSIONS

We have summarized various white and colored impulsive noise models that are commonly used in the literature. These are shown to be ineffective in modeling the dependence between observations in snapping shrimp data sets. Further analysis reveals that scatter plots between delayed samples depict near-elliptical geometries. Based on this observation and the fact that α -sub-Gaussian distributions are elliptical, the $\alpha\text{SGN}(m)$ model is proposed. Not only is this model able to track the empirical amplitude distribution but also offers elliptical distributions between closely spaced samples. We further highlight how the model can be represented by a Markov chain. In our results, we tune the $m+2$ parameters of the $\alpha\text{SGN}(m)$ model to snapping shrimp data sets. The tuned model, clearly offers better proximity than other impulsive noise models commonly used in the literature.

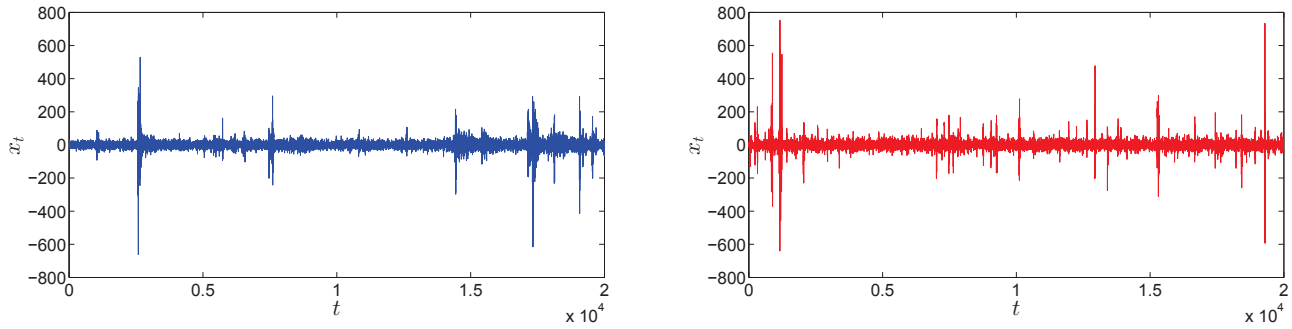


Fig. 9. For \mathcal{D}_2 : Empirical observations (left) and a realization of $\alpha\text{SGN}(4)$ (right) with tuned parameters.

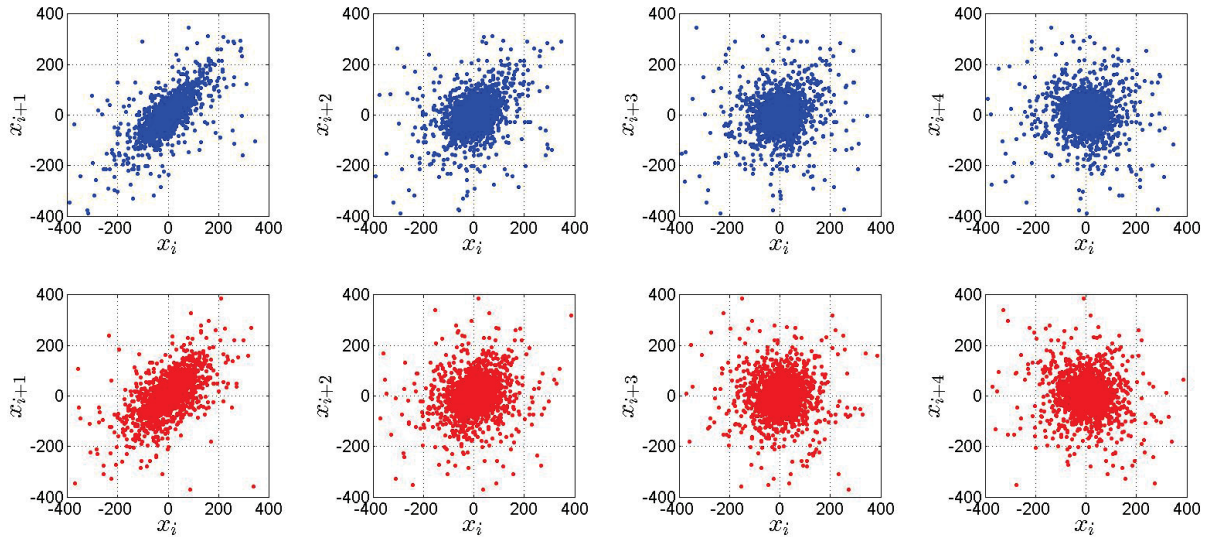


Fig. 10. For \mathcal{D}_2 : Delay scatter plots (top row) and those of the tuned $\alpha\text{SGN}(4)$ realization (bottom row).

REFERENCES

- [1] M. W. Legg, "Non-gaussian and non-homogeneous poisson models of snapping shrimp noise," Ph.D. dissertation, Curtin Univ. of Technology, 2009.
- [2] W. W. L. Au and K. Banks, "The acoustics of the snapping shrimp *synalpheus parneomeris* in kaneohe bay," *The J. of the Acoustical Soc. of Amer.*, vol. 103, no. 1, pp. 41–47, 1998.
- [3] A. Mahmood, "Digital communications in additive white symmetric alpha-stable noise," Ph.D. dissertation, Natl. Univ. of Singapore, June 2014.
- [4] M. Ghosh, "Analysis of the effect of impulse noise on multicarrier and single carrier QAM systems," *IEEE Trans. Commun.*, vol. 44, no. 2, pp. 145–147, Feb. 1996.
- [5] D. Middleton and I. for Telecommun. Sciences, *Statistical-physical Models of Man-made and Natural Radio Noise*, ser. OT report. U.S. Department of Commerce, Office of Telecommunications, 1974, no. pt. 2.
- [6] M. Chitre, J. Potter, and S.-H. Ong, "Optimal and near-optimal signal detection in snapping shrimp dominated ambient noise," *IEEE J. Ocean. Eng.*, vol. 31, no. 2, pp. 497–503, April 2006.
- [7] G. Samorodnitsky and M. S. Taqqu, *Stable Non-Gaussian Random Processes: Stochastic Models with Infinite Variance*. Chapman & Hall, 1994.
- [8] C. L. Nikias and M. Shao, *Signal processing with Alpha-Stable Distributions and Applications*. New York: Chapman-Hall, 1996.
- [9] J. Proakis and M. Salehi, *Digital Communications*, ser. McGraw-Hill higher education. McGraw-Hill Education, 2007.
- [10] D. Middleton, "Statistical-physical models of electromagnetic interference," *IEEE Trans. Electromagn. Compat.*, vol. EMC-19, no. 3, pp. 106–127, 1977.
- [11] A. Papoulis and U. S. Pillai, *Probability, Random Variables and Stochastic Processes*. Boston: McGraw-Hill, Dec 2001.
- [12] D. Fertonani and G. Colavolpe, "On reliable communications over channels impaired by bursty impulse noise," *IEEE Trans. Commun.*, vol. 57, no. 7, pp. 2024–2030, July 2009.
- [13] G. Ndo, F. Labeau, and M. Kassouf, "A markov-middleton model for bursty impulsive noise: Modeling and receiver design," *IEEE Trans. Power Del.*, vol. 28, no. 4, pp. 2317–2325, Oct 2013.
- [14] J. Nolan, "Maximum likelihood estimation and diagnostics for stable distributions," in *Lévy Processes*, O. Barndorff-Nielsen, S. Resnick, and T. Mikosch, Eds. Birkhuser Boston, 2001, pp. 379–400. [Online]. Available: http://dx.doi.org/10.1007/978-1-4612-0197-7_17
- [15] S. Kring, S. Rachev, M. Hchsttter, and F. Fabozzi, "Estimation of α -stable sub-gaussian distributions for asset returns," in *Risk Assessment*, ser. Contributions to Econ. Physica-Verlag HD, 2009, pp. 111–152.